ARTICLE

Dependence of Surface Facet Period on the Diameter of Nanowires

Fang Li, Peter D. Nellist, Christian Lang, and David J. H. Cockayne*

Department of Materials, University of Oxford, Parks Road, Oxford, OX1 3PH, U.K.

ABSTRACT Axial heterostructured silicon nanowires with varying *n*- and *p*-doping were synthesized using a vapor—liquid—solid approach. The nanowire sidewalls exhibit periodic nanofaceting in the silicon deposited directly on the sidewalls when diborane dopant gas is introduced during growth. For such nanofaceting, a model predicting the distance between facets (the facet period) is developed. For a nanowire structure, an extra energy cost term arising from the formation of apexes between facets is considered, and the facet size is predicted to decrease as the wire diameter increases. It is found that the model fits the experimental data well, and the fitted parameters in the model lie within the ranges of their expected values.

KEYWORDS: silicon · nanowire · facet · surface · transmission electron microscopy

One-dimensional (1D) semiconductor nanostructures have stimulated great interest in the last few decades, owing to their importance in fundamental scientific research and potential technological applications.[1] Being one of the most important 1D semiconductor nanostructures, silicon nanowires (SiNWs) have gained considerable attention, as they could become one of the basic building blocks of future nanoscale devices, including transistor components,[2,3] chemical/biological detectors,[4] and nanoelectromechanical systems.[5] The successful integration of SiNWs into devices depends ultimately on their microstructural control, which can be achieved through the growth optimization. For example, owing to the high surface area to volume ratio of nanowires, the surface plays an important role in controlling nanowire properties, and one issue of particular importance is the good control of the surface structure of wires. Recently nanoscale periodic faceting on nanowire sidewalls has been reported,[6−9] caused by regular twinning,[6] Au-rich clusters on the SiNW sidewalls,[7] absence of stable orientation parallel to the wire growth direction,[8] or dopant impurities deposited during the enhanced sidewall growth.[9] Therefore, to precisely control the nanowire growth to achieve desired surfaces for nanowire-based devices, it is crucially important to understand the nanowire faceting mechanisms and factors that influence faceting.

Faceting of a planar surface and its corresponding mechanisms are long-standing problems in materials science and surface physics.[10−12] Broadly, faceting can be understood in terms of the lowering of surface energy by the reconstruction of a surface into facets with lower surface energy, despite the resulting increase in surface area. A simple consideration of surface energies, however, does not predict the period of the facets on a surface. For a fully faceted surface under steady state conditions, the total surface area for each facet is fixed no matter what facet size distribution there is. It has been previously shown[13] that the period of faceting results from a competition between the energy cost of forming the edges of the facets and an energy term arising from the surface stress force monopoles at the edges. This is because the edge formation energy cost drives toward long facet periods with fewer edges, while the energy arising from the surface stress force monopoles partially cancels as the edges get closer together thereby driving toward a shorter facet period. While existing models for surface faceting can reliably predict facet period on planar surface,[14] they fail in the case of nanowire sidewalls. In this paper we develop a thermodynamic model for the facet period in a nanowire structure where the situation is complicated by the high curvature of the surface. A good match of the model with experimental data is observed for physically reasonable parameters.

*Address correspondence to david.cockayne@materials.ox.ac.uk.

Received for review October 16, 2009 and accepted January 18, 2010.

Published online January 29, 2010. 10.1021/nn901428u

RESULTS AND DISCUSSION

Axially doped nanowire heterostructures with *p*-type (B-doped), *n*-type (P-doped), and intrinsic Si were synthesized using a vapor−liquid−solid (VLS) method. The synthesized SiNWs are axially oriented along ⟨111⟩, having diameters in the range of 30−250 nm. Periodic nanofaceting is observed on all six Si{112} sidewall surfaces in the Si that is directly deposited on the sidewalls during the B-doped growth, while both the P-doped and the intrinsic SiNW regions exhibit a smooth surface morphology. The crystallographic planes on which the nanofaceting occurs are determined to be {111} and {100}.[9] These observations have led us to investigate the phenomenon of sidewall faceting in 1D nanostructures in general.

To understand the faceting on the surfaces of a nanowire, we assume that the wire diameter is 2*r* and the cross section is a regular hexagon before faceting occurs, with the length of each side of the hexagon being *r*, and the facet period being *L* (Figure 1A). Following Shchukin *et al.*[14] and considering the periodic faceting on one of the six nanowire sidewalls (it is the same for the other five sidewalls), the total free energy *f* of the faceted nanowire sidewall per unit projected area is given by

$$f = f_{surf} + E_{boundaries} + E_{elastic} \quad (1)$$

where f_{surf} is the surface free energy of all facets on the sidewall, $E_{boundaries}$ is the energy for forming edges and apexes at facet boundaries, and $E_{elastic}$ is the elastic energy due to the discontinuity of the surface stress tensor at the crystal edges.[15] Here the surface free energy f_{surf} can be expressed as

$$f_{surf} = c_1\gamma_{\{111\}}^{\ 0} + c_2\gamma_{\{100\}}^{\ 0} \quad (2)$$

where $\gamma_{\{111\}}^{\ 0}$ and $\gamma_{\{100\}}^{\ 0}$ are the surface tensions of the {111} and {100} facets, respectively, and c_1 and c_2 are constants. Because the interplanar angles between Si{112}, {111}, and {100} planes are fixed, the surface area of either the {111} or the {100} facet is proportional to that of the original (unfaceted) {112} SiNW sidewall (Figure 1B).

For a nanowire structure, $E_{boundaries}$ should include the energy of the edges formed between facets of different orientations on one sidewall, and the energy of apexes and sidewall boundaries formed when facets on neighboring sidewalls meet. Thus the energy of boundaries per unit projected area is given by

$$E_{boundaries} = 2\frac{\eta}{L} + 2\frac{B}{rL} + \frac{2c_3\eta_1 + c_4\eta_2}{r} \quad (3)$$

The first term in eq 3 is the edge formation energy per unit projected area, where η is the free energy cost per unit length of creating an edge between {111} and {100} facets on one sidewall. For a nanowire structure,

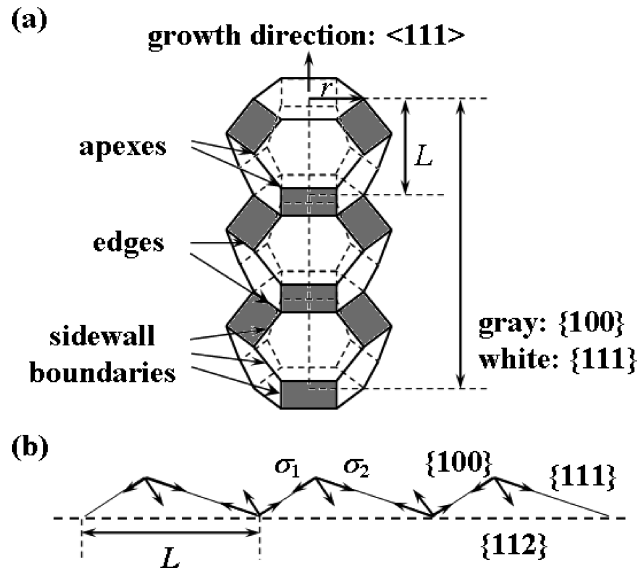

Figure 1. (a) Schematic of the three-dimensional structure of a faceted axial heterostructured SiNW in the B-doped region; and (b) schematic of the two-dimensional periodic faceting occurred on a SiNW sidewall surface. Force monopoles due to surface stress tensor discontinuity appear at edges.

when facets on neighboring sidewalls meet, apexes are formed (see Figure 1A). The second term in eq 3 is the apex formation energy per unit projected area, where *B* is the free energy due to the facet interactions at the apex. The projected area of faceted sidewall is proportional to *r*, whereas the number of apexes is independent of *r*, so the apex energy per unit area is inversely proportional to *r*. The multiplier 2 in the first and second terms of eq 3 is because there are on average two edges and two apexes formed within the axial length of one facet period *L*. When facets on neighboring sidewalls meet, the sidewall boundaries are also formed. As seen from Figure 1A, within the axial length of one facet period *L*, there are two boundaries formed between the {111} and {100} facets on neighboring sidewalls, and one boundary between the adjacent {111} facets. Thus the third term in eq 3 describes the energy of these sidewall boundaries, where η_1 and η_2 are the free energy costs per unit length for forming the sidewall boundaries between {111} and {100} facets and the boundaries between the adjacent {111} facets on neighboring sidewalls, respectively. Here c_3 and c_4 are constants, because the interplanar angles between Si{112}, {111}, and {100} planes are fixed, the length of the sidewall boundaries is proportional to the axial length of the nanowire.

The third term in eq 1, $E_{elastic}$, describes the elastic relaxations of the surface: when alternating facets coexist on the surface, neighboring facets have different values of the intrinsic surface stress tensor σ_1 and σ_2 (Figure 1B). Because of this intrinsic surface stress tensor discontinuity, effective force monopoles are created at the edges between two adjacent facets (Figure 1B). Following Alerhand *et al.*,[15] the elastic relaxation energy

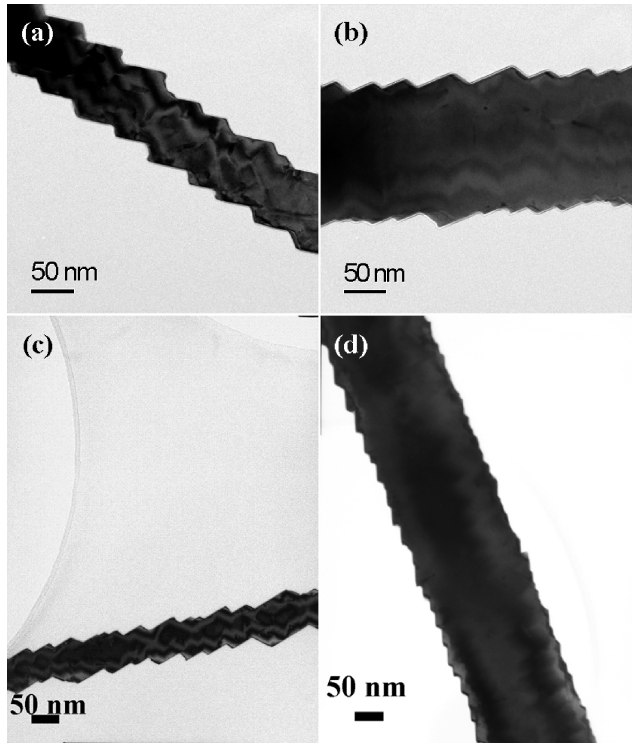

Figure 2. TEM images of several ⟨111⟩-oriented SiNWs in the faceted B-doped region with different wire diameters of (a) ~60; (b) ~145; (c) ~50; and (d) ~175 nm. (All are viewed along the ⟨110⟩ zone axis.)

depends logarithmically on the period L of the structure:

$$E_{\text{elastic}} = -\frac{g}{L}\ln\left(\frac{L}{b\pi}\right) \quad (4)$$

where g is a quantity calculated from the Young's modulus, Poisson's ratio, and surface stress tensor of crystalline Si, as defined in ref 15, and b is an atomic cutoff for the continuum elastic theory on the order of a lattice constant of Si. By substituting eqs 2−4 into eq 1, one obtains the following expression for the free energy of the faceted nanowire surface per unit projected area:

$$f = (c_1\gamma_{\{111\}}{}^0 + c_2\gamma_{\{100\}}{}^0) + \left[2\frac{\eta}{L} + 2\frac{B}{rL} + \left(\frac{2c_3\eta_1 + c_4\eta_2}{r}\right)\right] - \frac{g}{L}\ln\left(\frac{L}{b\pi}\right) \quad (5)$$

f has a minimum when the period of faceting L is

$$L = b\pi\exp\left(2\frac{\eta}{g} + 1 + \frac{4B}{g2r}\right) \quad (6)$$

As seen from eq 6, only the term in the argument of the exponential that arises from the apex energy is dependent on wire diameter, $2r$, and becomes increasingly important at small diameter, such as in a nanowire system. The facet period L is a function of the wire diameter $2r$, and L decreases as the wire diameter increases. To test this prediction, we used a transmission electron microscope (TEM) to observe several ⟨111⟩-oriented SiNWs in the faceted B-doped region. Figure 2A−D shows the TEM images of several ⟨111⟩-oriented faceted SiNWs with different wire diameters, taken along the ⟨110⟩ zone axis. The measured average facet periods are 61 ± 4, 56 ± 2, 51 ± 3, and 50 ± 3 nm, for the SiNW with the diameter of ~50 (Figure 2C), ~60 (Figure 2A), ~145 (Figure 2B), and ~175 nm (Figure 2D), respectively. It is seen that the average facet period decreases as the wire diameter increases. This is in accordance with the prediction from the model. In Figure 3, the measured average facet period L is shown as a function of the wire diameter $2r$. A nonlinear least-squares fit of eq 6 to these data is shown, with the values derived from fitting being $\eta/g = 1.153 \pm 0.006$ and $B/g = 26.8 \pm 2.0$ Å. g is evaluated to be in the range of 0.009−0.011 eV/Å, by calculating the surface stress tensor with the Young's modulus and Poisson's ratio of Si measured under the different measurement conditions.[16,17] Therefore, the ranges of the values of edge energy η and apex energy B are calculated to be $0.010 \pm (5.4 \times 10^{-5})$ to $0.013 \pm (6.6 \times 10^{-5})$ eV/Å and 0.24 ± 0.02 to 0.29 ± 0.02 eV, respectively. These values derived from fitting are in surprisingly good agreement with the reported edge energy η scattered in the range of 0.001−0.024 eV/Å and B scattered in the range of 0.06−0.3 eV.[16,18,19]

The observed (as well as predicted) dependence of facet period on wire diameter is different from the linear relationship observed experimentally by Ross *et al.*[8] in the *in situ* TEM observation of the faceting on intrinsic SiNW surfaces during ultrahigh vacuum (UHV)-VLS growth. The difference is likely to be due to the different mechanisms of the nanowire growth and faceting formation. Ross *et al.*[8] interpreted the faceting they observed as resulting from the interplay of the geometry and surface energies of the wire and liquid droplet. In the work presented here, heterostructured SiNWs with axially varying doping are not grown under UHV conditions, and the nanofaceting occurs during the enhanced sidewall growth that arises when the diborane dopant gas is introduced,[9] rather than from instabilities

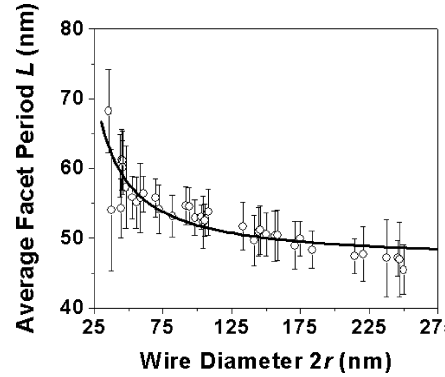

Figure 3. The dependence of average facet period on the wire diameter of the ⟨111⟩-oriented axial heterostructured SiNWs in the faceted B-doped region. The solid line through the data points is the nonlinear least-squares fit to the eq 6.

in the liquid droplet at the primary growth front, as suggested in Ross's model.[8] As such, our model describes the thermodynamic equilibrium structure with a term arising from the apex energy that becomes significant on surfaces with nanoscale radii of curvature. Our model has been developed assuming a regular hexagonal cross-section for the nanowires. High resolution scanning electron microscope images presented in ref 9 show that this is a reasonable approximation for the nanowires in the present study. Truncated hexagons have also been observed under different growth conditions.[8] The theoretical model presented here can be readily adapted to truncated hexagon cross sections by noting that the hexagon sides, while still being proportional to *r*, are not exactly equal to *r*. In addition, we emphasize that this model does not apply to SiNWs with very small diameters. Although no thin SiNWs with diameters less than 30 nm are observed in the current study, we note that many aspects of small-diameter nanowire sidewall faceting (should they exist) are beyond the scope of the discussion in the paper. It has been suggested[20] that the growth behavior of ultrathin nanowires (diameter $<$ 10 nm) can be totally different from the classical VLS growth of large-diameter nanowires. If facets do occur on the sidewalls of such ultrathin nanowires, a different faceting model should come into play. In addition, the growth direction of the VLS-grown SiNWs depends strongly on the wire diameter, *i.e.*, the small-diameter ($<$ *ca.* 20 nm) SiNWs are ⟨110⟩ oriented, while SiNWs with diameters larger than 40 nm normally grow along ⟨111⟩, and those with intermediate diameters grow along ⟨112⟩.[21] For nanowires growing in different directions, the shapes of the cross section as well as the sidewall orientations are different. Therefore, the facets (if there are any) occurring on the sidewalls of non-⟨111⟩ oriented SiNWs will be different from those on the ⟨111⟩-oriented SiNW sidewalls. A different faceting mechanism will apply to SiNWs in the small-diameter region.

CONCLUSIONS

We have developed a thermodynamic model of periodic surface faceting for the high curvature surfaces of a nanowire structure, and shown that the facet period is wire diameter dependent. This model consistently explains the experimentally observed dependence of facet size on wire diameter in the boron-dopant induced nanofaceting on SiNW sidewalls in the VLS-grown SiNWs, and quantitatively fits the experimental data with independently established values for the apex and edge energy parameters. We note that the model presented here predicts the thermodynamic equilibrium faceting period because we have minimized the free energy. It is of course the case that nanowire growth can be considered as a kinetically controlled process. Our previous study[9] showed that the observed faceting occurs in the Si that is directly deposited on the sidewalls by a vapor−solid mechanism catalyzed by the diborane gas present, and is therefore not kinetically constrained. It is also likely that the stress induced by the B impurities enhances surface diffusion allowing the equilibrium faceting period, predicted by the model presented here, to be found.

METHODS

Heterostructured SiNWs with axially varying *n*- and *p*-doping were grown by the VLS approach using gold as the catalyst in a FirstNano EasyTube3000 low pressure chemical vapor deposition system. SiNW growth was initiated by flowing silane gas, and the SiNWs were either *p*- or *n*-doped by introducing diborane or phosphine gas, respectively, to form the axial heterostructured B-doped/P-doped/intrinsic SiNWs. The detailed growth parameters have been reported previously.[9] After growth, the samples were removed from the growth substrates by sonication in acetone. The suspension was then drop cast onto a TEM finder grid covered with a 20 nm holey carbon film for TEM characterization. TEM imaging was made using a JEOL 2000FX TEM operating at 200 kV.

Acknowledgment. We acknowledge the University of Oxford and the U.K. Engineering and Physical Sciences Research Council for a scholarship (F.L.).

REFERENCES AND NOTES

1. Hu, J.; Odom, T. W.; Lieber, C. M. Chemistry and Physics in One Dimension: Synthesis and Properties of Nanowires and Nanotubes. *Acc. Chem. Res.* **1999**, *32*, 435–445.
2. Goldberger, J.; Hochbaum, A. I.; Fan, R.; Yang, P. Silicon Vertically Integrated Nanowire Field Effect Transistors. *Nano Lett.* **2006**, *6*, 973–977.
3. Cui, Y.; Lieber, C. M. Functional Nanoscale Electronic Devices Assembled Using Silicon Nanowire Building Blocks. *Science* **2001**, *291*, 851–853.
4. Li, Z.; Chen, Y.; Li, X.; Kamins, T. I.; Nauka, K.; Williams, R. S. Sequence-Specific Label-Free DNA Sensors Based on Silicon Nanowires. *Nano Lett.* **2004**, *4*, 245–247.
5. He, R.; Yang, P. Giant Piezoresistance Effect in Silicon Nanowires. *Nat. Nanotechnol.* **2006**, *1*, 42–46.
6. Johansson, J.; Karlsson, L. S.; Svensson, C. P. T.; Mårtensson, T.; Wacaser, B. A.; Deppert, K.; Samuelson, L.; Seifert, W. Structural Properties of ⟨111⟩ B-oriented III−V Nanowires. *Nat. Mater.* **2006**, *5*, 574–580.
7. Hannon, J. B.; Kodambaka, S.; Ross, F. M.; Tromp, R. M. The Influence of the Surface Migration of Gold on the Growth of Silicon Nanowires. *Nature* **2006**, *440*, 69–71.
8. Ross, F. M.; Tersoff, J.; Reuter, M. C. Sawtooth Faceting in Silicon Nanowires. *Phys. Rev. Lett.* **2005**, *95*, 146104.
9. Li, F.; Nellist, P. D.; Cockayne, D. J. H. Doping-Dependent Nanofaceting on Silicon Nanowire Surfaces. *Appl. Phys. Lett.* **2009**, *94*, 263111.
10. Mullins, W. W. Theory of Linear Facet Growth During Thermal Etching. *Phil. Mag.* **1961**, *6*, 1313–1341.
11. Flytzani-Stephanopoulos, M.; Schmidt, L. D. Morphology and Etching Processes on Macroscopic Metal Catalysts. *Prog. Surf. Sci.* **1979**, *9*, 83–111.
12. Williams, E. D.; Bartelt, N. C. Thermodynamics of Surface Morpology. *Science* **1991**, *251*, 393–400.
13. Rousset, S.; Repain, V.; Baudot, G.; Ellmer, H.; Garreau, Y.; Etgens, V.; Berroir, J. M.; Croset, B.; Sotto, M.; Zeppenfeld, P.; *et al.* Self-Ordering on Crystal Surfaces: Fundamentals and Applications. *Mater. Sci. Eng., B* **2002**, *96*, 169–177.

14. Shchukin, V. A.; Bimberg, D. Spontaneous Ordering of Nanostructures on Crystal Surfaces. *Rev. Mod. Phys.* **1999**, *71*, 1125–1171.
15. Alerhand, O. L.; Vanderbilt, D.; Meade, R. D.; Joannopoulos, J. D. Spontaneous Formation of Stress Domains on Crystal Surfaces. *Phys. Rev. Lett.* **1988**, *61*, 1973–1976.
16. Stewart, J.; Goldenfeld, N. Spinodal Decomposition of a Crystal Surface. *Phys. Rev. A* **1992**, *46*, 6505–6512.
17. França, D. R.; Blouin, A. All-Optical Measurement of In-Plane and Out-of-Plane Young's Modulus and Poisson's Ratio in Silicon Wafers by Means of Vibration Modes. *Meas. Sci. Technol.* **2004**, *15*, 859–868.
18. Hannon, J. B.; Bartelt, N. C.; Swartzentruber, B. S.; Hamilton, J. C.; Kellogg, G. L. Step Faceting at the (001) Surface of Boron-Doped Silicon. *Phys. Rev. Lett.* **1997**, *79*, 4226–4229.
19. Bartelt, N. C.; Tromp, R. M. Low-Energy Electron Microscopy Study of Step Mobilities on Si(001). *Phys. Rev. B* **1996**, *54*, 11731–11740.
20. Wang, N.; Cai, Y.; Zhang, R. Q. Growth of Nanowires. *Mater. Sci. Eng., R* **2008**, *60*, 1–51.
21. Wu, Y.; Cui, Y.; Huynh, L.; Barrelet, C. J.; Bell, D. C.; Lieber, C. M. Controlled Growth and Structures of Molecular-Scale Silicon Nanowires. *Nano Lett.* **2004**, *4*, 433–436.